ELSEVIER

Journal of Power Sources 89 (2000) 176–179

JOURNAL OF POWER SOURCES

www.elsevier.com/locate/jpowsour

Addition of a thin-film inorganic solid electrolyte (Lipon) as a protective film in lithium batteries with a liquid electrolyte

Nancy J. Dudney *

Solid State Division, Oak Ridge National Laboratory P.O. Box 2008, Oak Ridge, TN 37831-6030, USA

Received 2 November 1999; accepted 10 February 2000

Abstract

Three rechargeable lithium cells have been fabricated using thin films of Li and sputter-deposited $Li_xMn_{2-y}O_4$ as the electrodes, and a $LiPF_6$ organic liquid electrolyte. Cells were cycled up to 18 times between 4.5 and 2.5 V at 25°C both with and without the addition of the thin-film lithium phosphorus oxynitride solid electrolyte, known as Lipon. Of the cells tested, the Lipon film was most effective in maximizing the capacity and cycling efficiency when deposited in direct contact with the cathode; however, a significant improvement over the Lipon-free cell was also observed with Lipon sandwiched between layers of the liquid electrolyte. In the latter case, the Lipon was deposited onto a microporous polypropylene separator membrane. Published by Elsevier Science S.A.

Keywords: Lipon; Lithium batteries; Liquid electrolyte

1. Introduction

Thin-film all solid-state rechargeable lithium batteries have been fabricated at ORNL using an amorphous lithium phosphorous oxynitride electrolyte, known as Lipon. The stability of these batteries at high voltage and over long cycle times has been attributed to the electrochemical stability of the Lipon films. In this paper, preliminary results are presented exploring the potential advantage of adding Lipon films to lithium battery systems, which use a liquid or polymer electrolyte. In this way, Lipon might function as a stable protective solid electrolyte interphase film (SEI) preventing reaction between the anode or cathode materials and the electrolyte. The biggest obstacle is that the Lipon must be deposited under vacuum onto a reasonably smooth surface, free of micrometer-size pores or crevices, in order to achieve a continuous thin film. The submicron porous separator membranes used in many batteries offer such a vacuum compatible and smooth surface that can be coated with Lipon. Some anode and cathode sheets may also present an accommodating surface for the Lipon deposition if smooth and free of volatile components.

2. Background

The electrochemical and physical properties of the Lipon electrolyte films have been presented in earlier publications [1] and are summarized in Table 1. Typical compositions vary from $Li_{3.3}PO_{3.8}N_{0.24}$ to $Li_{3.6}PO_{3.3}N_{0.69}$. The small amount of N in the structure is essential to enhance both the Li^+ ion conductivity and the electrochemical stability window over those observed for films of Li_3PO_4. When deposited on a suitable substrate, 1-μm thick films are single phase, X-ray amorphous, dense, and free of pores and cracks.

Several cathode materials have been used to form thin-film lithium batteries at ORNL, including $LiCoO_2$, V_2O_5, and $LiMn_2O_4$ [2–4]. In this study, the cathode films are sputter-deposited $Li_xMn_{2-y}O_4$ [5]. These unannealed cathodes are X-ray amorphous, however TEM examination indicates that the films are at least partially nanocrystalline. Thin-film lithium batteries made with this cathode have a high specific capacity between 4.5 and 2.5 V and

* Corresponding author. Tel.: +1-423-576-4874; fax: +1-423-574-4143.

E-mail address: dudneynj@ornl.gov (N.J. Dudney).

0378-7753/00/$ - see front matter. Published by Elsevier Science S.A.
PII: S0378-7753(00)00427-4

Table 1
Properties of lipon electrolyte thin-films

Conductivity	2 (±1) μS/cm
Li^+ transference number	1.0
Density	2.5 g/cm^3
Electrochemical stability	0 to 5.5 V vs. Li metal
Thermal stability	≥ 300°C (in dry Ar)

can be recharged thousands of times with little decrease in cell capacity. Prolonged cycling especially at 100°C, however, leads to a gradual increase in the crystallinity of the cathode film.

3. Experimental

The Lipon electrolyte films were deposited by RF magnetron sputtering from a Li_3PO_4 target in a N_2 process gas as described in earlier publications [1–3]. For this study, films were deposited simultaneously onto several pieces of polypropylene membrane, ~25 μm thick, (Celgard 3401) and onto one of the thin-film $Li_xMn_{2-y}O_4$ cathodes. At a process pressure of 20 mTorr N_2 and a film deposition rate of 13 Å/m, the substrate holder was <42°C during the entire deposition. The Lipon films were 2 cm^2 by 1.5 μm thick.

The cathode and anode for the cells were also prepared as thin films by techniques used for our all solid-state batteries [2–4]. Each electrode was deposited onto a separate Ni coated polycrystalline alumina substrate (Coors, Lustrasurf, ADS-996). The cathode was $Li_xMn_{2-y}O_4$ deposited by sputtering from a $LiMn_2O_4$ target under conditions that typically give a dense film with a Mn-deficient film composition [5]. Cathode films were 1 cm^2 by 0.25 μm thick. The lithium metal anodes, 1 cm^2 by 3 μm thick, were deposited under vacuum from a thermal evaporation source.

The cells were assembled by sandwiching two layers of the liquid electrolyte saturated polypropylene membranes between the anode and cathode films on the Ni-coated alumina substrates. Each cell configuration is given in Table 2 where ''liq.E'' designates a liquid electrolyte layer within a single thickness of the polypropylene membrane. Two of these separator layers were used to avoid pressing the Lipon film against a hard electrode surface. The assembly was clipped together and placed in a sealed container to minimize evaporative loss of the electrolyte. The cells were assembled in a high purity Ar-filled glove box (<1 ppm H_2O and O_2). The electrolyte, 1 M $LiPF_6$ in ethylene carbonate (45 wt.%) + dimethyl carbonate (55 wt.%) (Grant Chemicals) was dispensed in the glove box from a stainless pressure vessel. The water and HF concentrations reported by the manufacturer's analysis was 17 and 19 ppm.

Table 2
Battery configurations

Cell A	Ni|Li|liq.E, liq.E|Lipon|$Li_xMn_{2-y}O_4$|Ni
Cell B	Ni|Li|liq.E, liq.E|$Li_xMn_{2-y}O_4$|Ni
Cell C	Ni|Li|liq.E|Lipon|liq.E|$Li_xMn_{2-y}O_4$|Ni

The batteries were evaluated using a Maccor battery test system equipped with 1 mA, 5 V, high impedance test channels. For each cycle, the batteries were charged at constant current and then held at 4.5 V until the current decreased to <1 μA or until the charging time exceeded 5 h. The cells were discharged at constant current to a 2.5-V cut-off voltage followed by an immediate recharge. Examination of the cathode, Lipon and anode films was done in the JEOL scanning electron microscope equipped with a Tracor Northern energy dispersive X-ray spectrometer.

4. Result and discussion

The initial charge and first five discharge curves at different current densities for Cell A are shown in Fig. 1a.

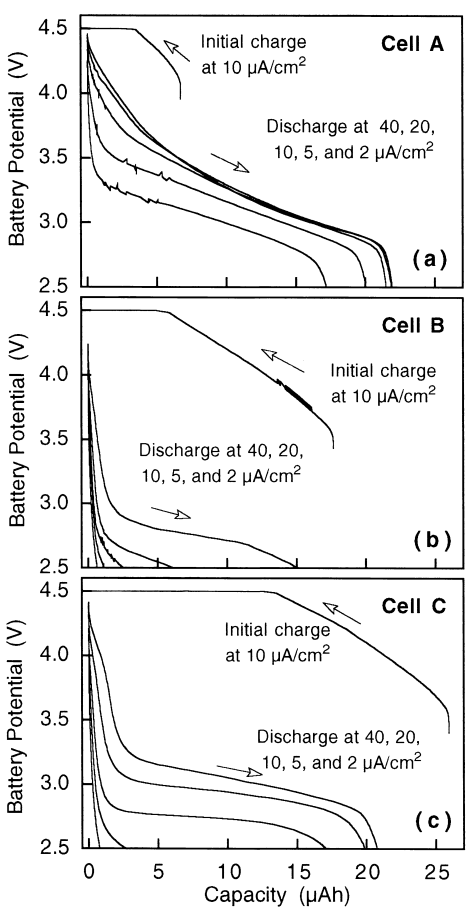

Fig. 1. The initial charge cycle and first five discharge cycles recorded at the specified current densities for Cells A, B, and C. Cells were recharged at 20 μA/cm^2 with a hold at 4.5 V (not shown).

Although the curves are noisier, the shapes of the charge and discharge curves are quite similar to those reported for our all solid-state lithium cells with the X-ray amorphous $Li_xMn_{2-y}O_4$ cathodes [5]. The cell resistance, judged by the suppression of the cell potential with increasing current densities, is also comparable to that for the solid-state cells being dominated by the resistance to lithium diffusion within the cathode film. There are two small but notable deviations from behavior for the all solid-state cells. The observed capacity of this cell, ~ 210 μA h/mg, is somewhat larger than expected for this voltage range from our liquid-free batteries (143 ± 23 μA h/mg), and the ratios of the discharge capacity to the subsequent charge capacity, Cd/Cc, for cycles 1 to 5 are 0.97 to 1.0, which are slightly lower. Within experimental error, the Cd/Cc ratio, also referred to as the cycle efficiency, is always 1.0 for our solid-state thin-film lithium batteries. Both of these comparisons indicate that reactions involving the liquid electrolyte and the Li anode or Lipon are likely occurring, which do not occur for the all solid-state system.

Fig. 1b and c show the same charge and discharge curves for Cells B and C in which the liquid electrolyte is in direct contact with the cathode film. The difference in the initial open circuit voltage for these cells compared to that of Cell A suggests that a reaction between the cathode and liquid electrolyte has occurred prior to the passage of any current through the cell. Both the shape of the discharge curves and the capacities of cells B and C reflect a much higher internal cell resistance than that of Cell A, which is most likely due to a corrosion layer at the cathode interface. The cell capacity for different current densities is shown more clearly in Fig. 2. Finally, although not illustrated in the plotted results, the charge required upon the charge cycle always exceeds that realized from the previous discharge by at least 1 to 6 μA h.

Results of subsequent cycling are shown in Fig. 3a and b. For these cycles, the cells were discharged at 5 μA/cm^2 and recharged at 20 μA/cm^2 with the usual hold at 4.5 V. Cell A has both the highest capacity and the highest cycle efficiency, and shows no significant deterioration after the initial five cycles. Likewise, Cell C shows no appreciable capacity fade, but this cell has a much lower cycle efficiency, ~ 0.8. Cell B shows a gradual increase in capacity and efficiency, but levels off to the lowest cycle efficiency requiring an additional 10 μA h to charge the cell over that realized from the cell discharge. The constant Cc/Cd ratio indicates that, whatever secondary reactions are occurring within these cells, these reactions show no sign of approaching completion.

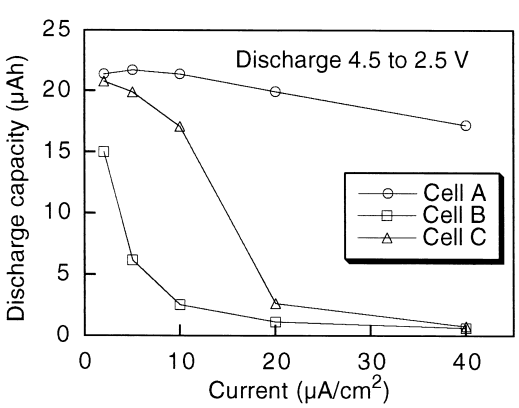

Fig. 2. Discharge capacity for the 4.5 to 2.5 V discharge curves of Fig. 1 plotted as a function of the current density.

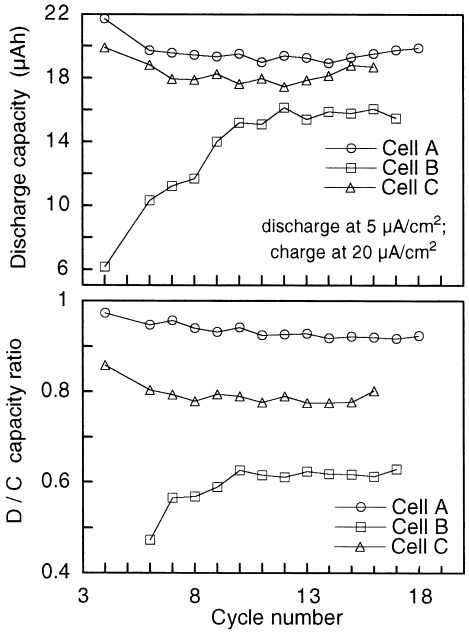

Fig. 3. Discharge capacity (top) and the cycle efficiency (bottom) for each cell upon continuous cycling over an additional 6 days. Current densities were 5 and 20 μA/cm^2 for the discharge and charge, respectively.

Each of the individual discharge curves for cycles 4 to 16, 17, or 18 are plotted in Figs. 4a–c. Here once again, Cell A is clearly the most stable one, while the shapes of the discharge curves for Cells B and C evolve during the cycling. Discharge curves for Cell C, in particular, are similar to those observed over hundreds of cycles of our solid-state cells. For the solid-state cells, there is evidence that growth of the nanocrystalline grains during cycling increased the capacity at above 3.8 V as more of the lithium can occupy the well-ordered spinel lattice sites. It is reasonable that the fluid electrolyte in contact with the cathode may enhance the rate of such a recrystallization.

Following the 16–18 cycles, the cells were disassembled and examined. With the exception of cell B, each of the cathode, Lipon, and Li films appeared unchanged. The lithium films maintained their shiny silver appearance with no evidence of dendritic or mossy growths. The lithium film of cell B, however, appeared blotchy being visibly darkened over much of the area. Energy dispersive X-ray analysis revealed a small Mn contamination (K_α and K_β peaks) in the darker areas, as well as strong peaks due to the K_α emissions from F, P, and O. Precipitation of Mn at

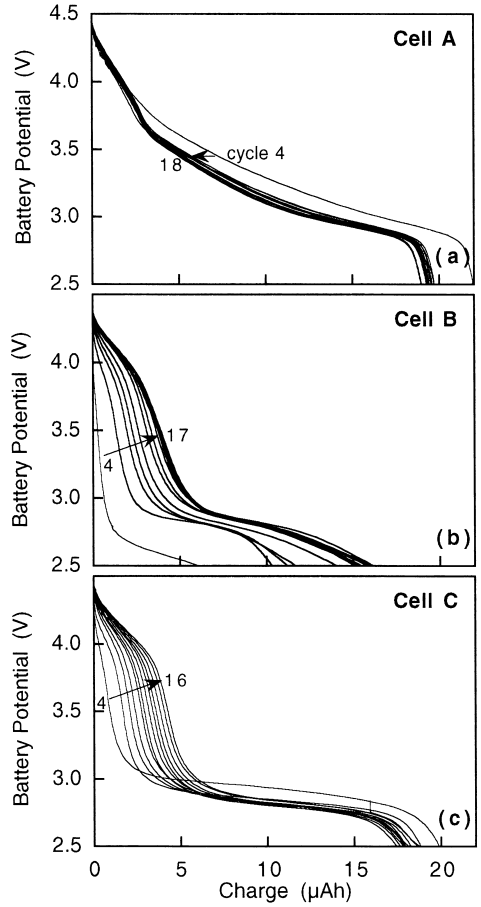

Fig. 4. Evolution of the discharge curves measured at 5 $\mu A/cm^2$. The cycle numbers are indicated in each figure.

the battery anode has been reported for a number of liquid and gel electrolyte cells and is considered one of the mechanisms responsible for the capacity fade [6]. The gradual dissolution of Mn from the cathode would also account for the observed saturation in the capacity above 3.8 V for the increasingly Mn-deficient Cell B (Fig. 4b), while the capacity at higher cell potential shown for Cell C (Fig. 4c) continues to expand with each cycle [7].

These results demonstrate that the presence of the Lipon electrolyte layer must be credited with inhibiting the diffusion and/or dissolution of the Mn cations. The excess charge capacities for each of the cells cannot be attributed solely to the Mn dissolution reaction. Other side reactions with the electrolyte components or impurities must account for the majority of the decreased cycling efficiency. It is interesting that the Lipon inserted within the liquid electrolyte reduces these reactions. This may be due to smaller concentration gradients within the liquid layers when separated by the Lipon film. Future experiments will utilize well-crystallized thin-film $Li_xMn_{2-y}O_4$ and $LiCoO_2$ cathodes cycled at higher current densities and will also explore the addition of Lipon at the electrolyte/anode interface.

5. Conclusions

Cycling experimental cells with a $LiPF_6$ in DMC + EC liquid electrolyte, nanocrystalline $Li_xMn_{2-y}O_4$ cathode and metallic Li anode demonstrate that the addition of a thin-film of the Lipon solid electrolyte enhances the stability, capacity and cycling efficiency of the cells. Of the cells tested, depositing the Lipon directly over the cathode is the most beneficial as this stabilized the cathode interface and avoids formation of a resistive reaction layer. Alternatively, the deposition of the Lipon film onto the porous separator membrane so that it can be inserted between two liquid electrolyte layers is also effective in reducing the undesirable side reactions attributable to the liquid electrolyte. In particular, a film of Lipon within the liquid electrolyte prevents the diffusion of Mn cations from the cathode to the lithium anode.

Acknowledgements

Research on thin-film batteries at ORNL has been supported by the US Department of Energy's Division of Materials Sciences, Division of Chemical Sciences, Office of Science, US Department of Energy under contract No. DE-AC05-96OR22464 with Lockheed Martin Energy Research.

References

[1] X. Yu, J.B. Bates, G.E. Jellison Jr., F.X. Hart, J. Electrochem. Soc. 144 (1997) 524.
[2] J.B. Bates, N.J. Dudney, B.J. Neudecker, B. Wang, Thin-film lithium batteries, in: T. Osaka, M. Datta (Eds.), New Trends in Electrochemical Technology: Energy Storage Systems in Electronics, Gordon & Breach, Newark, New Jersey, 2000, pp. 453–485.
[3] J.B. Bates, N.J. Dudney, D.C. Lubben, G.R. Gruzalski, B.S. Kwak, X. Yu, R.A. Zuhr, J. Power Sources 54 (1995) 58.
[4] www.ssd.ornl.gov/Programs/BatteryWeb/index.htm.
[5] N.J. Dudney, J.B. Bates, R.A. Zuhr, S. Young, J.D. Robertson, H.P. Jun, S.A. Hackney, J. Electrochem. Soc. 146 (1999) 2455.
[6] A. Blyr, C. Sigala, G. Amatucci, D. Guyomard, Y. Chabre, J.-M. Tarascon, J. Electrochem. Soc. 145 (1998) 194.
[7] T. Takada, H. Enoki, E. Akiba, T. Ishizu, T. Horiba, Mater. Res. Soc. Proc. 496 (1998) 257.